HHS Public Access

Author manuscript

Cancer Lett. Author manuscript; available in PMC 2016 August 28.

Published in final edited form as:

Cancer Lett. 2015 August 28; 365(1): 96–106. doi:10.1016/j.canlet.2015.05.016.

Antiproliferative effects of mitochondria-targeted cationic antioxidants and analogs: Role of mitochondrial bioenergetics and energy-sensing mechanism

Gang Cheng[a], **Jacek Zielonka**[a], **Donna McAllister**[a], **Micael Hardy**[b], **Olivier Ouari**[b], **Joy Joseph**[a], **Michael B. Dwinell**[c], and **Balaraman Kalyanaraman**[a,*]

[a]Department of Biophysics and Free Radical Research Center, Medical College of Wisconsin, 8701 Watertown Plank Road, Milwaukee, WI 53226 USA

[b]Aix-Marseille Université, CNRS, ICR UMR 7273, 13397 Marseille, France

[c]Department of Microbiology and Molecular Genetics, Medical College of Wisconsin, 8701 Watertown Plank Road, Milwaukee, WI 53226 USA

Abstract

One of the proposed mechanisms for tumor proliferation involves redox signaling mediated by reactive oxygen species such as superoxide and hydrogen peroxide generated at moderate levels. Thus, the antiproliferative and anti-tumor effects of certain antioxidants were attributed to their ability to mitigate intracellular reactive oxygen species (ROS). Recent reports support a role for mitochondrial ROS in stimulating tumor cell proliferation. In this study, we compared the antiproliferative effects and the effects on mitochondrial bioenergetic functions of a mitochondria-targeted cationic carboxyproxyl nitroxide (Mito-CP), exhibiting superoxide dismutase (SOD)-like activity and a synthetic cationic acetamide analog (Mito-CP-Ac) lacking the nitroxide moiety responsible for the SOD activity. Results indicate that both Mito-CP and Mito-CP-Ac potently inhibited tumor cell proliferation. Both compounds altered mitochondrial and glycolytic functions, and intracellular citrate levels. Both Mito-CP and Mito-CP-Ac synergized with 2-deoxy-glucose (2-DG) to deplete intracellular ATP, inhibit cell proliferation and induce apoptosis in pancreatic cancer cells. We conclude that mitochondria-targeted cationic agents inhibit tumor proliferation *via* modification of mitochondrial bioenergetics pathways rather than by dismutating and detoxifying mitochondrial superoxide.

*Corresponding author: (B. Kalyanaraman), Telephone: 414-955-4000; balarama@mcw.edu, Department of Biophysics and Free Radical Research Center, Medical College of Wisconsin, 8701 Watertown Plank Road, Milwaukee, WI 53226 USA.

Conflict of interest statement

None

Keywords

ROS; superoxide; mitochondria; tumor cell proliferation; antioxidant; 2-DG

1. Introduction

Reactive oxygen species (ROS), including superoxide ($O_2^{\bullet -}$) and hydrogen peroxide (H_2O_2), when generated at low picomolar levels, stimulate tumor cell proliferation [1–4]. Therefore, strategies to inhibit tumor proliferation include in part mitigation of intracellular ROS levels [5]. Exposure to higher levels of ROS as occurs in radiation or chemotherapy cause cytotoxicity in tumor cells due to oxidative damage to lipids, protein, and DNA. Reports suggest that antioxidant administration may interfere with the efficacy of radiation therapy or certain chemotherapy, or even enhance tumor progression by attenuating ROS levels in tumors [6,7].

Of the several sources of ROS generation pathways, membrane-associated NADPH oxidase (Nox) family of enzymes and mitochondria are recognized as major contributors of ROS in tumor cells [8,9]. More recently, we and others have shown that several structurally and functionally-distinct groups of mitochondria-targeted antioxidants [e.g., Mito-Q, triphenylphosphonium cation (TPP^+) conjugated to Co-Q; Mito-CP, TPP^+ conjugated to 3-carboxyproxyl nitroxide; Mito-Vitamin-E or Mito-chromanol, TPP^+ conjugated to Vitamin-E analog] inhibit tumor cell proliferation *in vitro* and attenuate tumor growth *in vivo* [10–13]. Previously, the antiproliferative effects of Mito-CP and related mitochondria-targeted antioxidants (MTAs) were attributed to ROS scavenging or superoxide dismutation mechanisms [14]. In this study we shed additional light on the antiproliferative mechanism of mitochondria-targeted antioxidants (containing TPP^+ moiety) in tumor cells. To this end, we compared the antiproliferative effects of Mito-CP, a mitochondria-targeted nitroxide exhibiting superoxide dismutase (SOD)-like activity with Mito-CP acetamide (Mito-CP-Ac), a newly-synthesized analog of Mito-CP lacking the nitroxide moiety and consequently, the SOD-like activity (see Fig. 1 for chemical structures). Results indicate that mitochondria targeted nitroxide (Mito-CP) and its redox-inactive analog (Mito-CP-Ac) inhibit tumor cell proliferation *via* a mechanism independent of superoxide dismutation mechanism in mitochondria, and that these compounds alter the bioenergetics pathways in tumor cells leading to inhibition of proliferation. The probes and methodology developed in this study also could be used as new tools with which the role of ROS in cancer cell proliferation can be investigated.

2. Materials and Methods

2.1. Chemicals

2-Deoxyglucose, potassium superoxide, dtpa, ferricytochrome *c*, Tempol, oligomycin, dinitrophenol, and antimycin A were purchased from Sigma-Aldrich (St. Louis, MO, USA). DIPPMPO spin trap was synthesized, as reported previously [15,16]. Mito-CP was synthesized according to the previously published procedure [17]. Mito-$Tempol_2$ was from

Cayman, and Mito-Tempol$_4$ was synthesized according to a modified procedure [18]. The synthetic pathway for Mito-CP-Ac is shown in Supplemental Figure 1.

2.2. Cell culture

MiaPaCa-2, PANC-1, MCF-7, MDA-MB-231, MCF-10A and A431 cell lines were obtained from the American Type Culture Collection (Manassas, VA, USA), where they were regularly authenticated. 253J bladder cancer cell line was a kind gift from Dr. William See (Department of Urology, Medical College of Wisconsin). Cells were stored in liquid nitrogen and used within 6 months after thawing. Details on cell culturing were previously reported [10,19,23].

2.3. Intracellular ATP measurements

Intracellular ATP levels were determined as previously shown [20] in cell lysates using a luciferase-based assay according to the manufacturer's instructions (Sigma-Aldrich).

2.4. OCR and ECAR assays

To determine the mitochondrial and glycolytic function in pancreatic cancer cells, we used the bioenergetics function assay, utilizing a Seahorse XF96 Extracellular Flux Analyzer (Seahorse Bioscience, North Billerica, MA, USA) [21,22]. Eight baseline oxygen consumption rate (OCR) and extracellular acidification rate (ECAR) measurements over 1 h were recorded after cell conditioning in the assay medium, and the values were averaged from the last six (most stable) readings. ECAR expressed as mpH/min was automatically converted to proton production rate (PPR) expressed as pmol H^+/min using the determined buffer capacity of the media and the chamber volume in XF96 Analyzer. The PPR-dependent changes are very similar to ECAR; however, we chose PPR instead of ECAR due to the ease of normalization, and to the logarithmic nature of ECAR with regard to the rate of production of H^+. OCR and ECAR (or PPR) values have been used as measures of mitochondrial respiration and glycolytic activity, respectively [23].

2.5. Clonogenic assay

The cells were seeded as indicated in six-well plates and treated with Mito-CP or Mito-CP-Ac for 24 h. The plates were kept within the incubator and media changed every 3-4 days until the control cells formed sufficiently large clones. The cell survival fractions were calculated as previously described [24].

2.6. IncuCyte Analyzer: Real time measurement of cell proliferation and apoptosis

The cell proliferation was measured using a label-free, non-invasive cellular confluence assay by IncuCyte Live-Cell Imaging Systems (Essen Bioscience, Ann Arbor, MI, USA). This system enables collection of live cell images at 2-h intervals over several days. The IncuCyte Analyzer provides real-time cellular confluence data based on segmentation of high-definition phase-contrast images. The cell proliferation is expressed as an increase in percentage of cell confluence [23].

The number of apoptotic cells was determined using the CellPlayer 96-well kinetic caspase-3/7 apoptosis reagent, which labels apoptotic cells green, according to the

manufacturer's instructions (Essen BioScience). Following indicated treatments, the plate was imaged using the IncuCyte Live-Cell Imaging Systems, and fluorescent images were taken every 2 h for up to 48 h.

The number of fluorescent objects was determined using the IncuCyte Software and was taken as the number of apoptotic cells. To measure the total cell number, at the endpoint of apoptosis assay, all of the samples in each treatment group were permeabilized by adding Triton × 100 (0.065%) in the presence of 0.2 μM Sytox Green (Invitrogen) as described previously [11] and the total number of green fluorescent objects per well was taken as 100%. The cell apoptosis is expressed as a percentage of apoptotic cells after normalization to total cell number for each group.

2.7. Immunoblotting

MiaPaCa-2 PDAC cells (1×10^6) were plated to 80% confluency in 60 mm dishes and then serum-starved for 5 hours. Stimulations with Mito-CP or Mito-CP-Ac were performed in serum-free medium. After stimulation, cells were washed twice in cold PBS and lysed using a modified RIPA buffer. Lysates were normalized for protein concentration, size separated using reducing SDS-PAGE, electro-transferred to PVDF membranes (Millipore) and then probed using primary and horseradish peroxidase-conjugated secondary antibodies. Antibodies against total or phosphorylated 5' AMP-activated protein kinase (AMPK) and Forkhead box M1(FOXM1) were purchased from Cell Signaling Technology (Danvers, MA) and used at the manufacturer's recommended dilutions. Proteins were visualized by chemiluminescence with auto-exposure and quantified by densitometric analysis using the FluorChem HD2 from Cell Biosciences (Santa Clara, CA). The optical densities of protein bands detected in immunoblots from independent experiments were obtained by densitometry.

2.8. Quantification of intracellular citrate by LC-MS/MS

Cells were grown on 10 cm dishes and treated with the compounds for 24 h in full medium. After incubation the cellular metabolism was quenched by rapid removal of the medium and washing the cells with freshly prepared ice-cold saline (0.9% NaCl in water). Cells were harvested in 1 ml of saline, a 40 μl aliquot of the suspension taken for the protein assay and the rest quickly centrifugated (1 min, 1,000 *g*). Supernatant was removed and the cell pellet placed on ice. To extract the intracellular citrate 1 ml of ice-cold mixture of water and acetonitrile (1:1) was added to the cell pellet, and the tube vortexed for 10 s, followed by incubation on ice for 10 min. Subsequently, tubes were quickly vortexed again and centrifugated (30 min, 20,000 *g*, 4 °C). Supernatant was passed through the SPE cartridge (Phree, Phenomenex) to remove phospholipids and the filtrate was frozen in liquid nitrogen and lyophilized overnight. The dry residue was stored in −80 °C freezer until the analysis. During the day of analysis the samples were reconstituted in ice-cold water (120 μl) by vortexing in a cold cabinet (5 min) and centrifugated (20 min, 20,000 *g*, 4 °C). The clear supernatants were transferred into HPLC vials and taken for LC-MS/MS analysis. LC-MS/MS analyses were performed using Kinetex C_{18} column (150 mm × 2.1 mm, 1.7 μm, Phenomenex) according to a method described elsewhere [25], with minor modifications. Briefly, the analyses were performed in a gradient mode using freshly prepared mobile

phase containing 10 mM tributylammonium acetate, pH 6.2 in water (mobile phase A) or in water:acetonitrile (1:1, mobile phase B). The column was equilibrated with a mixture containing 5% of mobile phase B and 95% of mobile phase A, at the flow rate of 0.4 ml/min. After sample injection the mobile phase B concentration was maintained at 5% for the first 2 min, and then raised to 100% over the next 22 min. Citrate was detected in the multiple reaction monitoring (MRM) mode using the transition of 191.0>87.0.

2.9. Quantification of intracellular Mito-CP and Mito-CP-Ac by LC-MS/MS

Cells were grown on 10 cm dishes and treated with the compounds for 24 h in full media. The protocol for Mito-CP and Mito-CP-Ac extraction from cells was the same as described previously for Mito-Vitamin E using dichloromethane:methanol (2:1) mixture, but without the addition of butylated hydroxytoluene (BHT) [11]. LC-MS/MS analyses were performed using Kinetex Phenyl-Hexyl column (50 mm × 2.1 mm, 1.7 μm, Phenomenex) equilibrated with water:acetonitrile mixture (4:1) containing 0.1% formic acid. Compounds were eluted by increasing the content of acetonitrile from 20% to 100% over 4 min and detected using MRM mode. Mito-CP and Mito-CP-Ac were selectively quantified based on MRM transitions of 601.2>586.2 and 628.2>415.2, respectively.

2.10. Statistical analysis

All results are expressed as the mean±S.D. Comparisons among groups of data were made using a one-way ANOVA with Turkey's *post hoc* analysis. A P-value <0.05 was considered to indicate statistical significance. The synergistic effects were confirmed by the combination index method.

3. Results

3.1. Superoxide dismutation by mitochondria-targeted and untargeted nitroxides and analogs in a chemical system

We determined the superoxide dismutation ability of compounds by monitoring their effects on the steady state concentrations of DIPPMPO-superoxide adduct (Fig. 2). DIPPMPO is a nitrone spin trap that reacts with superoxide to form a relatively persistent DIPPMPO-superoxide adduct (DIPPMPO-$^{\bullet}$OOH) [15]. Superoxide was generated by a slow-infusion (4 μl/min) of potassium superoxide (KO_2) solution in dimethylsulfoxide (DMSO) over a 10 min period. The flux of $O_2^{\bullet-}$ was calculated as 3.4 μM/min, as determined independently by monitoring the superoxide dismutase (SOD)-inhibitable reduction of ferricytochrome *c*. EPR analyses of incubations containing DIPPMPO (25 mM) and dtpa (0.1 mM) in phosphate buffer (pH 7.4, 50 mM) with a slow-infusion of KO_2 in DMSO over a 10 min period with continuous stirring generated spectra highly characteristic of the DIPPMPO-$^{\bullet}$OOH adduct [15] (Fig. 2A). The EPR parameters obtained based on computer simulation (Suppl. Table 1) are consistent with the published data for the DIPPMPO-$^{\bullet}$OOH adduct [15]. In the presence of small molecular weight nitroxides, Tempol and 3-carboxyproxyl (CP), the EPR spectrum of the DIPPMPO-$^{\bullet}$OOH adduct was almost completely abrogated (Fig. 2A). In the presence of Mito-CP, at the same concentration (1 mM), the spectral intensity of DIPPMPO-$^{\bullet}$OOH adduct was decreased by more than 50%. In contrast, Mito-CP-Ac, in which the superoxide-dismutating nitroxide moiety is replaced by an acetamidyl group, had no effect on the

DIPPMPO-•OOH adduct (Fig. 2A, *bottom*). Thus, Mito-CP-Ac lacks the ability to dismutate superoxide. The quantitative analyses of the relative concentrations of DIPPMPO-•OOH adduct obtained under various conditions show the differences in their ability to dismutate superoxide (Fig. 2C). Figures 2B and 2D show the same EPR spectra and their double integrations obtained at a much lower gain, indicating that the concentrations of the nitroxides used under the incubation conditions (cf. Fig. 2A) were nearly identical. From these results, we conclude that CP, Tempol, and Mito-CP to a lesser extent, can dismutate superoxide; however, as expected, Mito-CP-Ac with its nitroxide group changed to an acetamido group lacks the ability to dismutate $O_2^{\bullet -}$. Despite the differences in chemical structures and molecular masses, both compounds displayed very similar relative hydrophobicity, as indicated by nearly identical retention time during reversed phase separation on C_{18} column (Fig. 2E). Therefore we can expect similar uptake and intracellular distribution of Mito-CP and Mito-CP-Ac. In fact, as shown in Figure 2F, both Mito-CP and Mito-CP-Ac accumulated intracellularly to a similar level as detected by LC-MS. In addition, both compounds remained intact intracellularly, indicating that Mito-CP-Ac was not metabolized to Mito-CP in cells.

3.2. The antiproliferative effects of Mito-CP and Mito-CP-Ac in pancreas cancer cells

First, we used a clonogenic assay to monitor the antiproliferative effects of Mito-CP and Mito-CP-Ac (lacking the nitroxide group). As shown in Figure 3A (*top* and *bottom*), both agents dramatically decreased the colony formation and the survival fractions of MiaPaCa-2 cells at similar concentrations. Notably, this dramatic decrease in colony formation in MiaPaCa-2 cells was not observed in MCF-10A cells (non-tumorigenic mammary epithelial cells) when treated with either agent at the same low concentration. As the compounds do not undergo interconversion (Fig. 2F), the antiproliferative effects of both compounds are due to their individual effects.

Next, we confirmed the clonogenic results obtained for cancer cells by monitoring cell proliferation in real-time, using a label-free confluence assay by IncuCyte™ Live-Cell Imaging Systems. The IncuCyte Analyzer provides real-time updates on cell confluence, based on segmentation of high definition-phase contrast images. Changes in cell confluence were used as a surrogate marker of cell proliferation. Cells were seeded with different concentrations of Mito-CP or Mito-CP-Ac overnight in a 96-well plate. The cells were photographed and confluence calculated every 2 h by IncuCyte 2011A software. The inhibitory effects of Mito-CP and Mito-CP-Ac on cell proliferation in MiaPaCa-2 cells were shown to be nearly identical (Fig. 3B). The effects of Mito-CP and Mito-CP-Ac on the segmented high definition phase contrast images of cells are shown (Suppl. Fig. 2). Results from the two independent assays enabled us to conclude that both Mito-CP and Mito-CP-Ac are equipotent in inhibiting MiaPaCa-2 cell proliferation. Other nitroxides (e.g., Tempol) conjugated to the TPP^+ group also inhibited MiaPaCa-2 cell proliferation. However, the potency of the antiproliferative effect is dependent on the side chain length. Whereas Mito-$Tempol_2$ is relatively inert in MiaPaCa-2 cells at concentrations in the range of 0.01 to 1 μM, Mito-$Tempol_4$ (with a longer carbon-carbon side chain) is considerably more potent in inhibiting MiaPaCa-2 cell proliferation (Suppl. Fig. 3A). At up to 5 μM concentration

neither Mito-Tempol$_2$ nor Mito-Tempol$_4$ affected significantly intracellular ATP levels in MiaPaCa-2 cells (Suppl. Fig. 3B).

Previously, we had reported that Mito-CP combined with the glucose analog 2-deoxy-D-glucose (2-DG) synergistically depleted intracellular ATP levels in breast cancer cells [10]. We compared the ATP-depleting effects of Mito-CP and Mito-CP-Ac alone (Suppl. Fig. 3B) and in combination with different concentrations of 2-DG in MiaPaCa-2 cells (Fig. 3C). Both Mito-CP and Mito-CP-Ac had only modest effects on cellular ATP level when used alone at up to 5 μM concentrations, but synergized with 2-DG in a nearly identical manner in decreasing intracellular ATP levels. Furthermore, we compared the effects of Mito-CP and Mito-CP-Ac alone and in combination with different concentrations of 2-DG on apoptosis in MiaPaCa-2 cells (Suppl. Fig. 4 *top*). Both Mito-CP and Mito-CP-Ac had only minimal effects on apoptosis when used alone at up to 1 μM concentrations; at these concentrations the cell *proliferation* was already completely inhibited (Fig. 3). For comparison, gliotoxin exhibited strong pro-apoptotic effects under the same conditions. Both Mito-CP and Mito-CP-Ac synergized with 2-DG used at high concentration (10 mM) in a nearly identical manner in increasing apoptosis (Suppl. Fig. 4 *middle, bottom*). These results suggest that Mito-CP and Mito-CP-Ac target mitochondrial bioenergetics metabolism in pancreatic cancer cells.

We further confirmed that the antiproliferative effects of Mito-CP and Mito-CP-Ac also occur in other cancer cells, including breast and lung cancer cells (Fig. 4). Results obtained using the IncuCyte Analyzer show that both Mito-CP and Mito-CP-Ac exhibit similar dose- and time-dependent antiproliferative effects whether tested in pancreatic (MiaPaCa-2 and Panc-1), breast (MCF-7 and MDA-MB-231), lung (A431) or bladder (253J) cancer cells.

3.3. Effects of Mito-CP and Mito-CP-Ac on mitochondrial bioenergetics in MiaPaCa-2 cells

The oxygen consumption rate (OCR) and the extracellular acidification rate (ECAR) were measured as a readout of mitochondrial function and glycolysis using a Seahorse Bioscience XF96 extracellular flux analyzer [10,11,21,23]. We compared the bioenergetic functional changes in MiaPaCa-2 cells treated with Mito-CP and Mito-CP-Ac (Fig. 5A–C). Addition of varying concentrations of Mito-CP (Fig. 5B, *left*) and Mito-CP-Ac (Fig. 5B, *right*) dose-dependently decreased the oxygen consumption rate in an almost identical manner. Under these conditions, there was a compensatory increase in glycolysis or proton production rate (PPR) in MiaPaCa-2 cells treated with Mito-CP or Mito-CP-Ac. Figure 5A shows a two-dimensional representation of the changes in OCR and ECAR values in MiaPaCa-2 cells treated with various concentrations of Mito-CP and Mito-CP-Ac for 3 h and 24 h. During a 3 h treatment, both Mito-CP and Mito-CP-Ac inhibited OCR and elevated ECAR at similar concentrations (*dotted red line* in Fig. 5A). However, after a 24 h incubation period, Mito-CP and Mito-CP-Ac inhibited equally both OCR and ECAR under these conditions (*solid blue line* in Fig. 5A).These results suggest that the mechanism(s) by which Mito-CP and Mito-CP-Ac alter mitochondrial bioenergetics are similar.

Next we monitored the mitochondrial bioenergetics function in MiaPaCa-2 cells after treatment with Mito-CP or Mito-CP-Ac for 24 h followed by a washout of the treatments and return to fresh culture media. After a 24 h treatment with different concentrations, OCR

was measured and the effects of adding oligomycin (oligo), dinitrophenol (DNP), and rotenone plus antimycin A (Rot/AA) were determined (Fig. 5C). The use of these metabolic modulators enables determination of multiple parameters of mitochondrial function as reported previously [26]. Oligomycin was used to inhibit ATP synthase, DNP to uncouple mitochondria and yield maximal OCR, and AA to inhibit complex III and mitochondrial oxygen consumption. Based on the obtained results, it is apparent that both Mito-CP and Mito-CP-Ac inhibit ATP-linked OCR in MiaPaCa-2 cells. Previously, we have shown that the inhibitory effects on mitochondrial function elicited by Mito-CP are irreversible in MCF-7 breast cancer cells, whereas in MCF-10A (control, non-transformed) cells, the inhibition was abrogated with time after washout of Mito-CP [10]. It is therefore conceivable that Mito-CP-Ac also induces an irreversible mitochondrial inhibition in PDAC cells and a reversible effect in normal pancreatic cells.

3.4. Analysis of intracellular citrate levels by liquid chromatography-mass spectrometry: Metabolic reprogramming by Mito-CP and Mito-CP-Ac

Citric acid plays a central role in the metabolism and proliferation of cancer cells [27]. Therefore we determined the intracellular levels of citrate in MiaPaCa-2 cells treated with Mito-CP and Mito-CP-Ac and the results are shown in Figure 6A–B. There was a significant decrease in the steady state levels of citrate when cells were treated for 24 h with Mito-CP or Mito-CP-Ac (0.1 μM each). Similar or even stronger inhibitory effects were observed for both compounds when treated at 1 μM concentration over 3 h (*data not shown*). From these data it is clear that mitochondria-targeted cationic agents induce reprogramming of TCA metabolism, independent of their superoxide dismutation or general radical scavenging mechanism.

3.5. Effects of Mito-CP and Mito-CP-Ac on AMPK activation and FOXM1 expression

We next investigated whether mitochondria-targeted drugs induced 5' AMP-activated protein kinase (AMPK), a central metabolic regulator. AMPK activation was monitored in Mito-CP and Mito-CP-Ac treated MiaPaCa-2 cells. Human MiaPaCa-2 cells treated for up to 30 min with 1 μM of Mito-CP or Mito-CP-Ac were lysed, and proteins size-separated on SDS-page, transferred to PVDF, and probed with an antibody to phosphorylated AMPK Thr-172. As shown in Figure 6C, Mito-CP and Mito-CP-Ac treatment stimulated AMPK phosphorylation within 5 min. Cells treated with the oligomycin positive control demonstrated a similar level of AMPK activation. Similar dynamics of activation of the AMPK regulator by both compounds is consistent with the data obtained using the bioenergetics function (Fig. 5), and further suggests that the mitochondria-targeted cationic compounds downregulate cellular bioenergetics function and activate AMPK-sensing mechanism.

Next, we investigated the effects of Mito-CP and Mito-CP-Ac on Forkhead Box M1 transcription factor (FOXM1) expression in MiaPaCa2 cells. FOXM1, a redox-responsive transcription factor, regulates genes involved in S phase and the G2/M transition. Cells were incubated for 12 h with indicated concentrations of Mito-CP and Mito-CP-Ac and Western blotting was used to assay changes in protein expression. As shown in Figure 7, FOXM1 expression was significantly reduced in cells treated with Mito-CP and Mito-CP-Ac. These

results are consistent with AMPK activation data (Fig. 6C). However, a complete elucidation of the mechanistic pathway would require extensive investigation of downstream targets.

4. Discussion

4.1. Antiproliferative effects of mitochondria-targeted cationic agents in tumor cells

Lipophilic, delocalized cationic compounds that target tumor mitochondria because of a higher (more negative inside) mitochondrial membrane potential, as compared to normal cells [28,29], markedly inhibit mitochondrial function (*e.g.*, cell respiration) in cancer cells [10]. We previously reported that triphenylphosphonium cation (TPP^+)-linked agents conjugated to an aromatic or heterocyclic moiety exert selective cytostatic and cytotoxic effects in tumor cells [10,11]. Novel mitochondria-targeted cationic drugs that have been fine-tuned to sequester into mitochondrial matrix and membranes were synthesized in Murphy's and our laboratories [10,11,30]. Mitochondria-targeted cationic agents induce antiproliferative and cytotoxic effects in tumor cells without markedly affecting normal cells [10,11]. Mitochondria-targeted chromanols or Vitamin-E-like molecules inhibited breast tumor progression in xenograft models [11]. Previously, we reported that mitochondria-targeted chromanol (Mito-ChM) and its acetate ester analog (Mito-ChMAc) exhibit selective antiproliferative and cytotoxic effects in multiple breast cancer cells [11]. Although Mito-ChM (with an intact phenolic antioxidant group) and Mito-ChMAc (lacking the radical-scavenging phenolic hydroxyl group due to estrification) are equipotent in cancer cells, the intracellular hydrolysis of Mito-ChMAc to Mito-ChM suggests that the antiproliferative effects of MitoChMAc could conceivably be attributed to Mito-ChM [11]. In the present study, results show that Mito-CP-Ac does not undergo intracellular conversion to Mito-CP (Fig. 2F), thereby implicating that the antiproliferative effects are caused independently (albeit *via* a similar mechanism) in cancer cells. Although previous studies have linked ROS generation to antiproliferative and cytotoxic effects of mitochondria-targeted agents (Mito-Vitamin E succinate and Mito-curcumin) in cancer cells [31,32], convincing experimental support for this proposal is lacking. Spin-trapping measurements of ROS as a minor intermediate in cancer cells treated with cationic drugs should not be interpreted as a major mechanism of cancer cell death or inhibition of cancer cell proliferation [31,32].

4.2. Alterations in energy sensing and mitochondrial bioenergetics as a potential mechanism

Emerging research indicates development of new generation anticancer drugs targeting energy metabolism [33,34]. We reported that mitochondria targeted cationic drugs selectively inhibit ATP-linked mitochondrial respiration in tumor cells and potently activate AMP-activated protein kinase (AMPK) in human PDAC [23]. The AMPK signaling pathway has been studied extensively in cancer cell biology [35,36]. Other mitochondria-specific drugs (e.g., metformin) reportedly exert antitumor effects by elevating cellular AMP/ATP ratio and activating the AMPK pathway. AMPK, a master regulator of cellular energy homeostasis, is typically activated by elevation of cellular AMP [37]. Under increased cellular oxidative stress wherein ATP levels are decreased along with a concomitant increase in AMP (enhanced AMP-to-ATP ratio), AMPK is activated *via*

phosphorylation of its threonine-172 residue [38]. Previous research has shown that AMPK represses the FOXM1 transcription factor expression *via* inhibition of the AKT/FOXO3 signaling cascade, leading to regression of cervical cancer cell growth [39]. Treatment of lung cancer cells with Mito-CP resulted in the inhibition of FOXM1 [40]. This, combined with the possibility that Mito-CP and Mito-CP-Ac could activate AMPK and decrease FOXM1 expression, underscores the importance of the AKT/FOXO3/FOXM1 signaling pathway as a potential therapeutic target for mitochondria-targeted cationic drugs. It is likely that mitochondria-targeted cationic agents exert antiproliferative effects in cancer cells *via* targeting the energy sensing bioenergetics pathway(s).

4.3. Role of mitochondrial ROS in tumor proliferation

The role of ROS (superoxide and hydroxyl radicals, hydrogen peroxide) in tumor cell killing (e.g., radiation therapy) is well established [41]. However, the role of ROS (superoxide and hydrogen peroxide) in tumor cell proliferation still remains enigmatic, lacking convincing experimental proof [42]. Recently, we reported that mitochondria targeted antioxidants (Mito-CP, Mito-Q, and Mito-chromanols or Mito-Vit-E) selectively inhibit proliferation of multiple cancer cells [11]. In some cases, these effects were attributed to scavenging of mitochondria-derived ROS, resulting in the overall inhibition of tumor cell proliferation [13]. Both published results and the present data bring into question the significance of mitochondrial ROS in pancreatic cancer cell proliferation [11]. Blunting the antioxidant functions of Mito-CP (by changing the nitroxide group to an acetamido group) and Mito-chromanol (by estrification of the phenolic hydroxyl group) did not affect the antiproliferative effects of Mito-CP-Ac and Mito-chromanol acetate in several cancer cells [11]. Mito-CP and Mito-chromanol exhibit superoxide dismutating and radical scavenging abilities [16]. The fact that both Mito-CP ($O_2^{\bullet -}$ dismutating agent) and Mito-CP-Ac (lacking $O_2^{\bullet -}$ dismutating ability) mitigate tumor proliferation to the same extent argues against mitochondrial ROS intermediacy as a regulatory factor in tumor proliferation mechanism. However, it is clear that tumor heterogeneity should be taken into consideration for proper interpretation. Recent studies indicate metabolic heterogeneity among hypoxic cancer cells, and that hypoxic tumor cells contain a sub-population of non-Warburg respiring cells [43]. Previously, we have shown that Mito-CP and other mitochondria-targeted antioxidants inhibit Nox2 expression and activity in mice and inhibit nitration and carbonylation of proteins induced by NADPH oxidases (Nox) and inducible NOS [44,45]. Nox enzymes are emerging as a highly promising target for anticancer drug development [8,9]. Increasing evidence suggests that Noxderived ROS inhibits tumor apoptosis and stimulates tumor proliferation [8,9]. It is plausible that indirect inhibition of Nox enzymes by Mito-CP and Mito-CP-Ac contributes to inhibition of tumor cell proliferation.

In summary, the present results suggest that mitochondria-targeted cationic nitroxides and antioxidants inhibit tumor cell proliferation *via* a mechanism mostly independent of scavenging of mitochondrial ROS [45] and that modulation of cellular bioenergetics and energy sensing mechanisms are likely to be responsible for their antiproliferative effects in tumor cells.

Supplementary Material

Refer to Web version on PubMed Central for supplementary material.

Acknowledgements

This work was supported by grants from the NIH National Cancer Institute [5U01CA178960-02 (to M.B.D. and B.K.) and 5R01 CA152810-03 (to B.K.)].

Abbreviations

2-DG	2-Deoxyglucose
ECAR	extracellular acidification rate
Mito-CP	mitochondria-targeted cationic carboxyproxyl nitroxide
Mito-CP-Ac	acetamide analog of Mito-CP lacking SOD-like activity
MTAs	mitochondria-targeted antioxidants
OCR	oxygen consumption rate
PPR	proton production rate

References

1. Fruehauf JP, Meyskens FL Jr. Reactive oxygen species: a breath of life or death? Clin Cancer Res. 2007; 13:789–794. [PubMed: 17289868]
2. Trachootham D, Alexandre J, Huang P. Targeting cancer cells by ROS-mediated mechanisms: a radical therapeutic approach? Nat Rev Drug Discov. 2009; 8:579–591. [PubMed: 19478820]
3. Behrend L, Henderson G, Zwacka RM. Reactive oxygen species in oncogenic transformation. Biochem Soc Trans. 2003; 31:1441–1444. [PubMed: 14641084]
4. Shin SY, Lee JM, Lee MS, Jung H, Lee YH. Targeting cancer cells via the reactive oxygen species-mediated unfolded protein response with a novel synthetic polyphenol conjugate. Clin Cancer Res. 2014; 20:4302–4313. [PubMed: 24938523]
5. Liou G-Y, Storz P. Reactive oxygen species in cancer. Free Radic Res. 2010; 44:479–496. [PubMed: 20370557]
6. St. Clair DK, Jordan JA, Wan XS, Gairola CG. Protective role of manganese superoxide dismutase against cigarette smoke-induced cytotoxicity. J Toxicol Environ Health. 1994; 43:239–249. [PubMed: 7932852]
7. Sayin VI, Ibrahim MX, Larsson E, Nilsson JA, Lindahl P, Bergo MO. Antioxidants accelerate lung cancer progression in mice. Sci Transl Med. 2014; 6(221):221ra15.
8. Block K, Gorin Y. Aiding and abetting roles of NOX oxidases in cellular transformation. Nat Rev Cancer. 2012; 12:627–637. [PubMed: 22918415]
9. Sanchez-Sanchez B, Gutiérrez-Herrero S, López-Ruano G, Prieto-Bermejo R, Romo-González M, Llanillo M, Pandiella A, Guerrero C, Miguel JF, Sánchez-Guijo F, Del Cañizo C, Hernández-Hernández A. NADPH oxidases as therapeutic targets in chronic myelogenous leukemia. Clin Cancer Res. 2014; 20:4014–4025. [PubMed: 24833663]
10. Cheng G, Zielonka J, Dranka BP, McAllister D, Mackinnon AC Jr, Joseph J, Kalyanaraman B. Mitochondria-targeted drugs synergize with 2-deoxyglucose to trigger breast cancer cell death. Cancer Res. 2012; 72:2634–2644. [PubMed: 22431711]
11. Cheng G, Zielonka J, McAllister DM, Mackinnon AC Jr, Joseph J, Dwinell MB, Kalyanaraman B. Mitochondria-targeted vitamin E analogs inhibit breast cancer cell energy metabolism and promote cell death. BMC Cancer. 2013; 13:285. [PubMed: 23764021]

12. Starenki D, Park JI. Mitochondria-targeted nitroxide, Mito-CP, suppresses medullary thyroid carcinoma cell survival in vitro and in vivo. J Clin Endocrinol Metab. 2013; 98:1529–1540. [PubMed: 23509102]
13. Jain M, Rivera S, Monclus EA, Synenki L, Zirk A, Eisenbart J, Feghali-Bostwick C, Mutlu GM, Budinger GR, Chandel NS. Mitochondrial reactive oxygen species regulate transforming growth factor-β signaling. J Biol Chem. 2013; 288:770–777. [PubMed: 23204521]
14. Weinberg F, Hamanaka R, Wheaton WW, Weinberg S, Joseph J, Lopez M, Kalyanaraman B, Mutlu GM, Budinger GR, Chandel NS. Mitochondrial metabolism and ROS generation are essential for Kras-mediated tumorigenicity. Proc Natl Acad Sci USA. 2010; 107:8788–8793. [PubMed: 20421486]
15. Chalier F, Tordo P. 5-Diisopropoxyphosphoryl-5-methyl-1-pyrroline N-oxide, DIPPMPO, a crystalline analog of the nitrone DEPMPO: synthesis and spin trapping properties. J Chem Soc Perk T2. 2002; 12:2110–2117.
16. Hardy M, Poulhés F, Rizzato E, Rockenbauer A, Banaszak K, Karoui H, Lopez M, Zielonka J, Vasquez-Vivar J, Sethumadhavan S, Kalyanaraman B, Tordo P, Ouari O. Mitochondria-targeted spin traps: synthesis, superoxide spin trapping, and mitochondrial uptake. Chem Res Toxicol. 2014; 27:1155–1165. [PubMed: 24890552]
17. Dhanasekaran A, Kotamraju S, Karunakaran C, Kalivendi SV, Thomas S, Joseph J, Kalyanaraman B. Mitochondria superoxide dismutase mimetic inhibits peroxide-induced oxidative damage and apoptosis: role of mitochondrial superoxide. Free Radic Biol Med. 2005; 39:567–583. [PubMed: 16085176]
18. Dickey JS, Gonzalez Y, Aryal B, Mog S, Nakamura AJ, Redon CE, Baxa U, Rosen E, Cheng G, Zielonka J, Parekh P, Mason KP, Joseph J, Kalyanaraman B, Bonner W, Herman E, Shacter E, Rao VA. Mito-tempol and dexrazoxane exhibit cardioprotective and chemotherapeutic effects through specific protein oxidation and autophagy in a syngeneic breast tumor preclinical model. PLoS One. 2013; 8:e70575. [PubMed: 23940596]
19. Zimmerman NP, Roy I, Hauser AD, Wilson JM, Williams CL, Dwinell MB. Cyclic AMP regulates the migration and invasion potential of human pancreatic cancer cells. Mol Carcinog. 2015; 54:203–215. [PubMed: 24115212]
20. Dong LF, Freeman R, Liu J, Zobalova R, Marin-Hernandez A, Stantic M, Rohlena J, Valis K, Rodriguez-Enriquez S, Butcher B, Goodwin J, Brunk UT, Witting PK, Moreno-Sanchez R, Scheffler IE, Ralph SJ, Neuzil J. Suppression of tumor growth in vivo by the mitocan alpha-tocopheryl succinate requires respiratory complex II. Clin Cancer Res. 2009; 15:1593–1600. [PubMed: 19223492]
21. Dranka BP, Hill BG, Darley-Usmar VM. Mitochondrial reserve capacity in endothelial cells: The impact of nitric oxide and reactive oxygen species. Free Radic Biol Med. 2010; 48:905–914. [PubMed: 20093177]
22. Dranka BP, Zielonka J, Kanthasamy AG, Kalyanaraman B. Alterations in bioenergetic function induced by Parkinson's disease mimetic compounds: lack of correlation with superoxide generation. J Neurochem. 2012; 122:941–951. [PubMed: 22708893]
23. Cheng G, Zielonka J, McAllister D, Tsai S, Dwinell MB, Kalyanaraman B. Profiling and targeting of cellular bioenergetics: inhibition of pancreatic cancer cell proliferation. Br J Cancer. 2014; 111:85–93. [PubMed: 24867695]
24. Franken NA, Rodermond HM, Stap J, Haveman J, van Bree C. Clonogenic assay of cells in vitro. Nat Protoc. 2006; 1:2315–2319. [PubMed: 17406473]
25. Balcke GU, Kolle SN, Kamp H, Bethan B, Looser R, Wagner S, Landsiedel R, van Ravenzwaay B. Linking energy metabolism to dysfunctions in mitochondrial respiration--a metabolomics in vitro approach. Toxicol Lett. 2011; 203:200–209. [PubMed: 21402135]
26. Nicholls DG, Darley-Usmar VM, Wu M, Jensen PB, Rogers GW, Ferrick DA. Bioenergetic profile experiment using C2C12 myoblast cells. J Vis Exp. 2010; 46:pii2511.
27. Icard P, Poulain L, Lincet H. Understanding the central role of citrate in the metabolism of cancer cells. Biochim Biophys Acta. 2012; 1825:111–116. [PubMed: 22101401]
28. Nadakavukaren KK, Nadakavukaren JJ, Chen LB. Increased rhodamine 123 uptake by carcinoma cells. Cancer Res. 1985; 45:6093–6099. [PubMed: 4063967]

29. Kurtoglu M, Lampidis TJ. From delocalized lipophilic cations to hypoxia: blocking tumor cell mitochondrial function leads to therapeutic gain with glycolytic inhibitors. Mol Nutr Food Res. 2009; 53:68–75. [PubMed: 19072739]
30. Smith RA, Hartley RC, Murphy MP. Mitochondria-targeted small molecule therapeutics and probes. Antioxid Redox Signal. 2011; 15:3021–3038. [PubMed: 21395490]
31. Dong LF, Jameson VJ, Tilly D, Cerny J, Mahdavian E, Marín-Hernández A, Hernández- Esquivel L, Rodríguez-Enríquez S, Stursa J, Witting PK, Stantic B, Rohlena J, Truksa J, Kluckova K, Dyason JC, Ledvina M, Salvatore BA, Moreno-Sánchez R, Coster MJ, Ralph SJ, Smith RA, Neuzil J. Mitochondrial targeting of vitamin E succinate enhances its pro-apoptotic and anti-cancer activity via mitochondrial complex II. J Biol Chem. 2011; 286:3717–3728. [PubMed: 21059645]
32. Reddy CA, Somepalli V, Golakoti T, Kanugula AK, Karnewar S, Rajendiran K, Vasagiri N, Prabhakar S, Kuppusamy P, Kotamraju S, Kutala VK. Mitochondrial-targeted curcuminoids: a strategy to enhance bioavailability and anticancer efficacy of curcumin. PLoS One. 2014; 9:e89351. [PubMed: 24622734]
33. Rodríguez-Enríquez S, Gallardo-Pérez JC, Hernández-Reséndiz I, Marín-Hernández A, Pacheco-Velázquez SC, López-Ramírez SY, Rumjanek FD, Moreno-Sánchez R. Canonical and new generation anticancer drugs also target energy metabolism. Arch Toxicol. 2014; 88:1327–1350. [PubMed: 24792321]
34. Phan ML, Yeung SC, Lee MH. Cancer metabolic reprogramming: importance, main features, and potentials for precise targeted anti-cancer therapies. Cancer Biol Med. 2014; 11:1–19. [PubMed: 24738035]
35. Chen S, Zhu X, Lai X, Xiao T, Wen A, Zhang J. Combined cancer therapy with non-conventional drugs: all roads lead to AMPK. Mini Rev Med Chem. 2014; 14:642–654. [PubMed: 25138094]
36. Kuhajda FP. AMP-activated protein kinase and human cancer: cancer metabolism revisited. Int J Obes (Lond). 2008; 32(Suppl 4):S36–S41. [PubMed: 18719597]
37. Hardie DG. AMPK: positive and negative regulation, and its role in whole-body energy homeostasis. Curr Opin Cell Biol. 2014; 33C:1–7. [PubMed: 25259783]
38. Emerling BM, Weinberg F, Snyder C, Burgess Z, Mutlu GM, Viollet B, Budinger GR, Chandel NS. Hypoxic activation of AMPK is dependent on mitochondrial ROS but independent of an increase in AMP/ATP ratio. Free Radic Biol Med. 2009; 46:1386–1391. [PubMed: 19268526]
39. Yung MM, Chan DW, Liu VW, Yao KM, Ngan HY. Activation of AMPK inhibits cervical cancer cell growth through AKT/FOXO3a/FOXM1 signaling cascade. BMC Cancer. 2013; 13:327. [PubMed: 23819460]
40. Cunniff B, Benson K, Stumpff J, Newick K, Held P, Taatjes D, Joseph J, Kalyanaraman B, Heintz NH. Mitochondrial-targeted nitroxides disrupt mitochondrial architecture and inhibit expression of peroxiredoxin 3 and FOXM1 in malignant mesothelioma cells. J Cell Physiol. 2013; 228:835–845. [PubMed: 23018647]
41. Cook JA, Gius D, Wink DA, Krishna MC, Russo A, Mitchell JB. Oxidative stress, redox, and the tumor microenvironment. Semin Radiat Oncol. 2004; 14:259–266. [PubMed: 15254869]
42. Glasauer A, Chandel NS. Targeting antioxidants for cancer therapy. Biochem Pharmacol. 2014; 92:90–101. [PubMed: 25078786]
43. Le A, Stine ZE, Nguyen C, Afzal J, Sun P, Hamaker M, Siegel NM, Gouw AM, Kang BH, Yu SH, Cochran RL, Sailor KA, Song H, Dang CV. Tumorigenicity of hypoxic respiring cancer cells revealed by a hypoxia-cell cycle dual reporter. Proc Natl Acad Sci USA. 2014; 111:12486–12491. [PubMed: 25114222]
44. Mukhopadhyay P, Horváth B, Zsengellér Z, Zielonka J, Tanchian G, Holovac E, Kechrid M, Patel V, Stillman IE, Parikh SM, Joseph J, Kalyanaraman B, Pacher P. Mitochondrialtargeted antioxidants represent a promising approach for prevention of cisplatin-induced nephropathy. Free Radic Biol Med. 2012; 52:497–506. [PubMed: 22120494]
45. Ghosh A, Kanthasamy A, Joseph J, Anantharam V, Srivastava P, Dranka BP, Kalyanaraman B, Kanthasamy AG. Anti-inflammatory and neuroprotective effects of an orally active apocynin derivative in pre-clinical models of Parkinson's disease. J Neuroinflammation. 2012; 9:241. [PubMed: 23092448]

Highlights

- Mitochondria-targeted antioxidants (MTAs) inhibit proliferation of cancer cells.
- Radical scavenging properties are not necessary for antiproliferative effects of MTAs.
- Inhibition of bioenergetic function is a common feature of different MTAs.

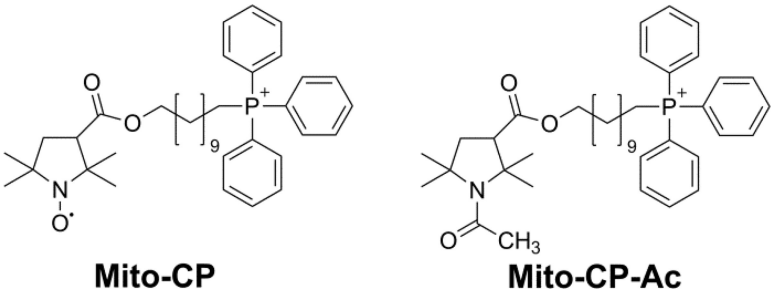

Fig 1. Chemical structures of Mito-CP and Mito-CP-Ac

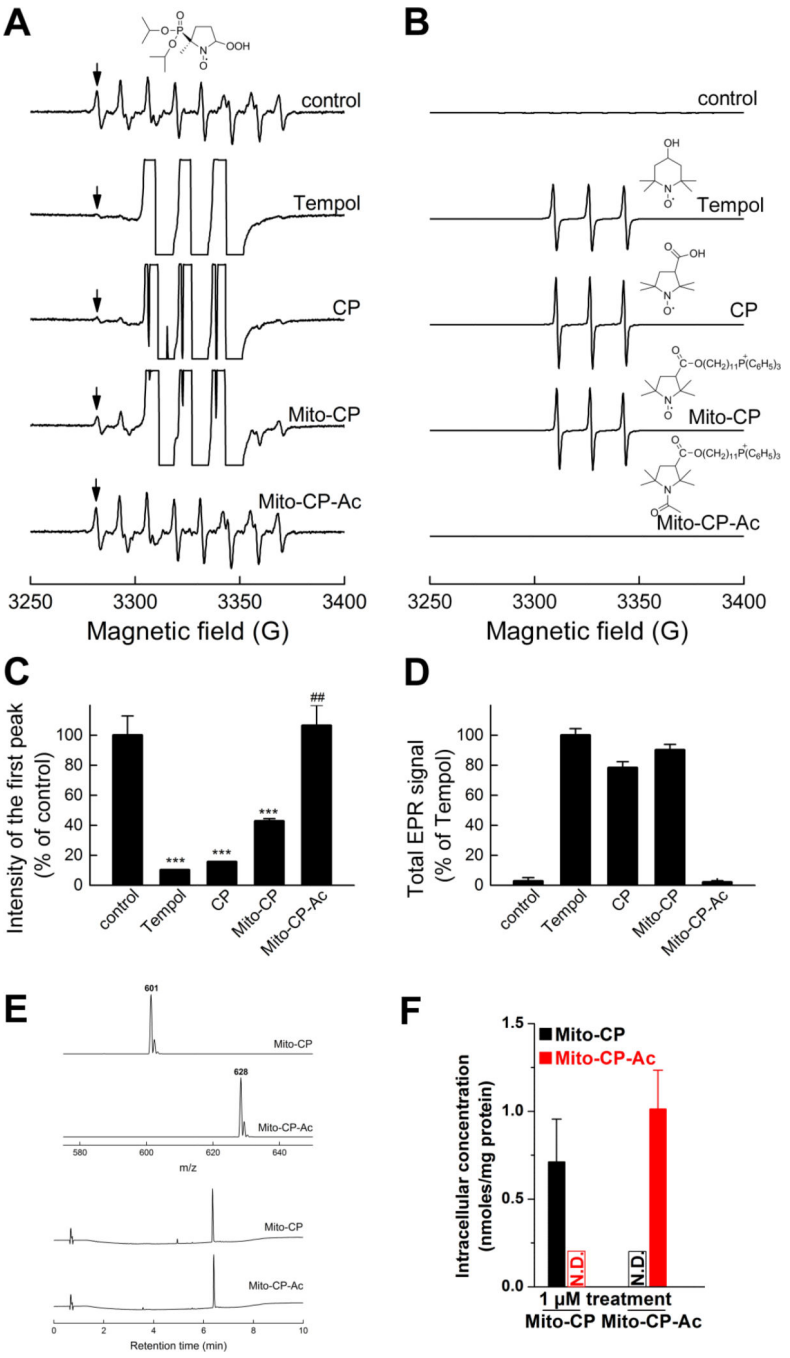

Fig. 2. Superoxide dismutation activity of Mito-CP and Mito-CP-Ac as determined by DIPPMPO-superoxide adduct formation

(A) EPR spectra collected during EPR spin trapping of superoxide radical anion. Control incubations contained DIPPMPO (25 mM), KO_2 in DMSO was slowly infused over 10 min into aqueous phosphate buffer (10 mM, pH 7.4) containing dtpa (100 μM). Where indicated, incubations contained Mito-CP (1 mM), Mito-CP-Ac (1 mM), Tempol (1 mM) or CP (1 mM). (B) Same as panel (A) but spectra were recorded at a lower receiver gain, so as to compare the concentrations of different nitroxides used. (C) Quantitative analyses of the DIPPMPO-•OOH adduct formed in various incubations, using the EPR intensity of the low

field line, as indicated by the arrows in panel A. *** $p < 0.001$ vs. control, ## $p < 0.01$ vs. Mito-CP. (D) Quantitative comparison of different nitroxides using the double integration of the spectra shown in panel B. (E) MS spectra (*top*) and HPLC traces (*bottom*) of synthesized Mito- CP and Mito-CP-Ac. (F) Intracellular concentrations of Mito-CP and Mito-CP-Ac in MiaPaCa-2 cells treated with 1 μM Mito-CP or Mito-CP-Ac for 24 h.

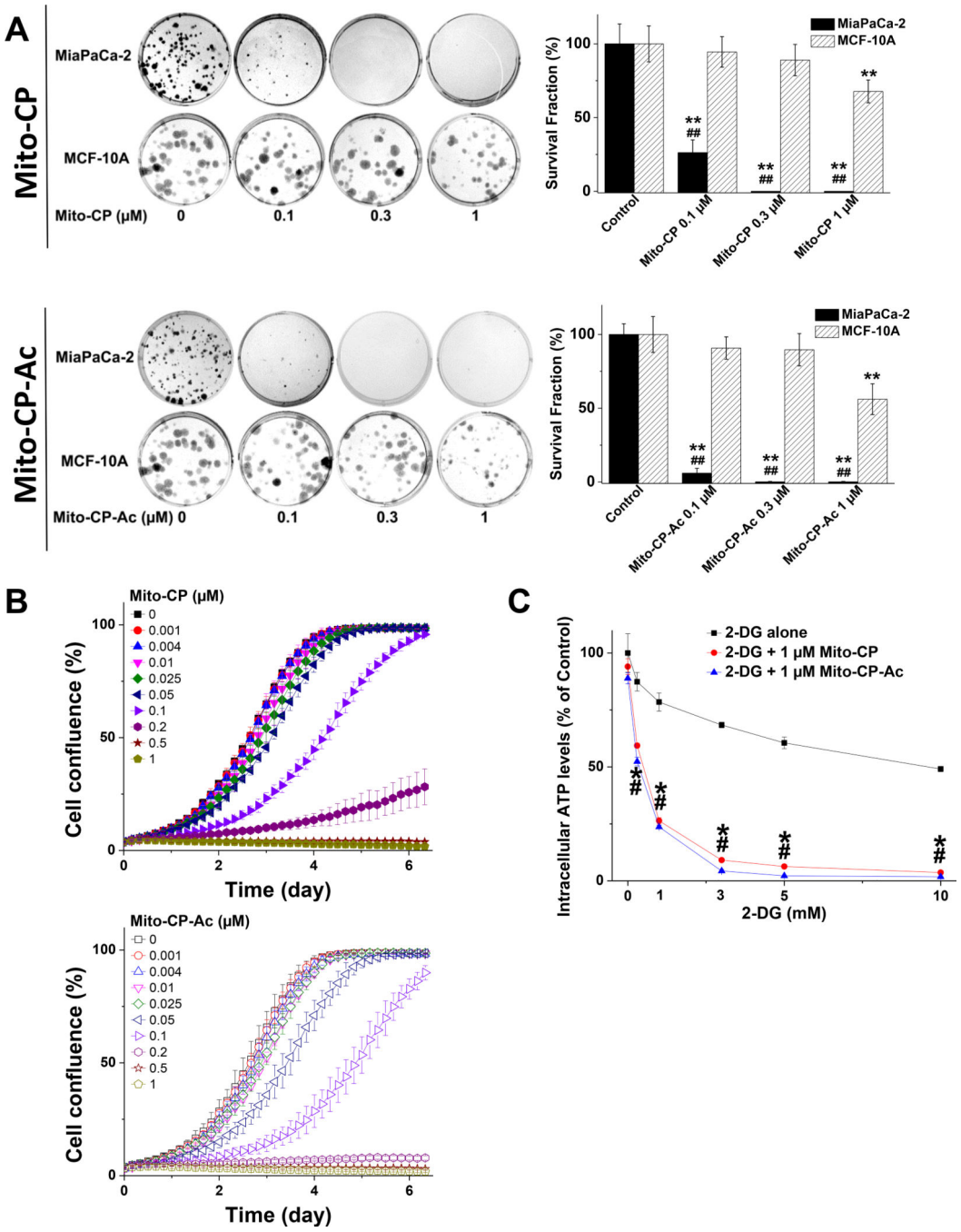

Fig. 3. Effects of Mito-CP or Mito-CP-Ac on colony formation, cell proliferation and intracellular ATP levels

(A) MiaPaCa-2 and MCF-10A cells were treated with Mito-CP (*top*) or Mito-CP-Ac (*bottom*) for 24 h and the colonies formed were counted after additional incubation. ** - $p < 0.01$ treatment vs. correspond control.## - $p < 0.01$, comparing MiaPaCa-2 with MCF-10A under the same treatment conditions.. (B) Effects of Mito-CP (*top*) or Mito-CP-Ac (*bottom*) at different concentrations on cell proliferation in MiaPaCa-2 cells. (C) Both Mito-CP and Mito-CP-Ac equally synergize with 2-DG to decrease intracellular ATP levels in MiaPaCa-2

cells. The cells seeded in 96-well plates were treated with 2-DG in the presence and absence of 1 μM of the Mito-CP or Mito-CP-Ac for 3 h. Data are represented as a percentage of control (untreated) cells after normalization to total protein for each well. The calculated absolute values of ATP after normalization to total protein for each well for MiaPaCa-2 control cells were 41 ± 3 nmol ATP/mg protein. $*,^{\#}$ - $p < 0.05$ for Mito-CP and Mito-CP-Ac vs. 2-DG alone, respectively. Data shown are the mean ± SD, n = 6 (panel A), n = 4 (panels B and C).

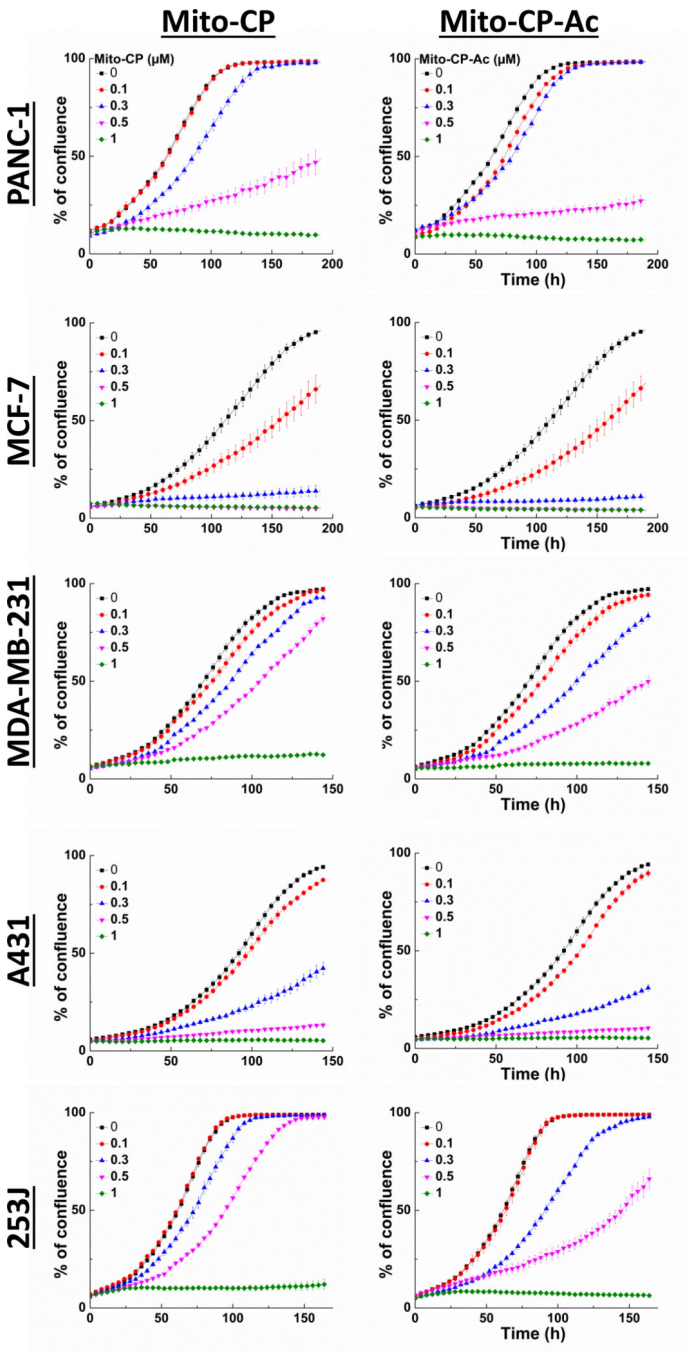

Fig. 4. Effects of Mito-CP and Mito-CP-Ac on proliferation in multiple cancer cell lines

Cell proliferation in PANC-1, MCF-7, MDA-MB-231, A431, and 253J cells was monitored in real-time with the continuous presence of indicated treatments until the end of each experiment. Data shown are the mean ± SD, n = 4.

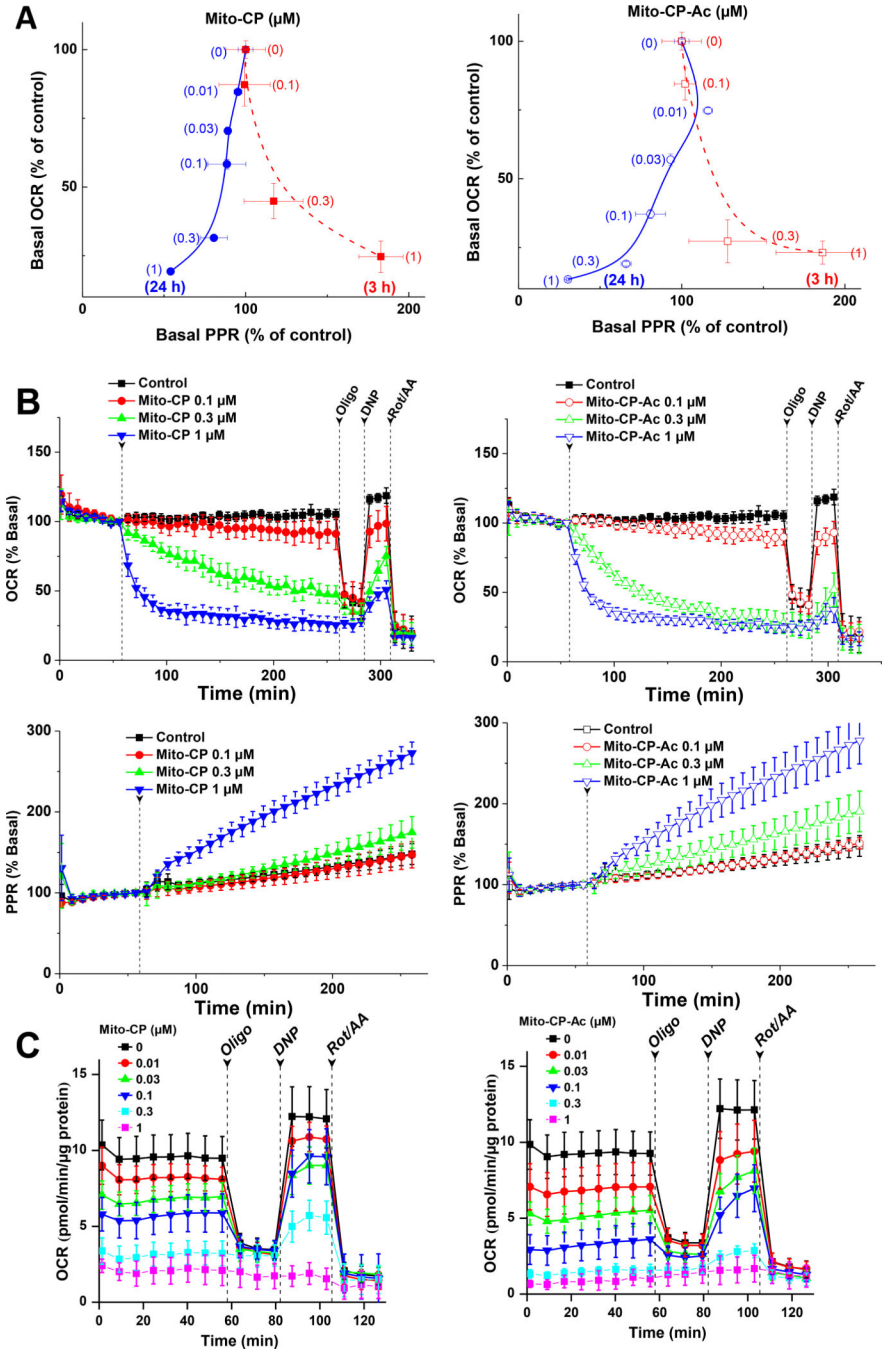

Fig. 5. Dose- and time-dependent effects of Mito-CP and Mito-CP-Ac on cell bioenergetic status, as shown in two-dimensional map of oxygen consumption rate (OCR) and proton production rate (PPR) measured in MiaPaCa-2 cells

(A) Two-dimensional bioenergetics map of OCR and ECAR at different concentrations of Mito-CP (*left panel*) and Mito-CP-Ac (*right panel*). (B) Effect of Mito-CP or Mito-CP-Ac in real time on OCR and PPR in MiaPaCa-2 cells. OCR and PPR were monitored in real time with Seahorse analyzer, and arrows indicate the time point of injection of compounds of interests. (C) Effect of 24 h treatment with Mito-CP or Mito-CP-Ac on OCR in MiaPaCa-2 cells.

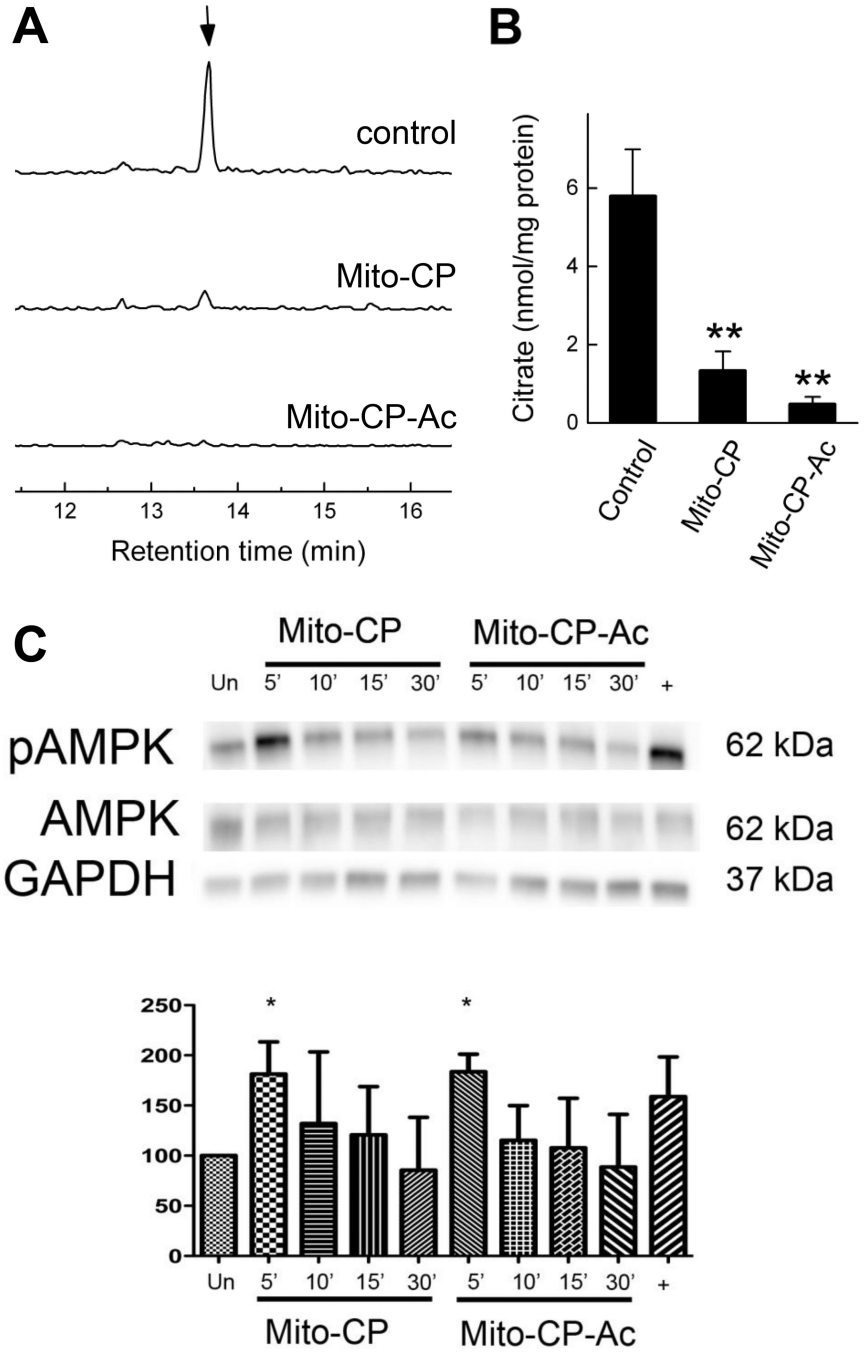

Fig. 6. Effect of Mito-CP and Mito-CP-Ac on intracellular level of citric acid and activation of AMPK in MiaPaCa-2 cells

(A) LC-MS/MS chromatograms corresponding to citrate (MRM 191.00>86.95). (B) Quantitative analysis of the effect of Mito-CP and Mito-CP-Ac on intracellular citrate levels. **- $p < 0.01$ vs. control. Cells were treated with 0.1 μM Mito-CP or Mito-CP-Ac for 24 h and analyzed as described in *Materials and Methods* section. (C) (*top*) The representative blot of three independent biological replicates of lysates obtained from MiaPaCa-2 cells stimulated for 5, 10, 15, or 30 min with equivalent doses of 1 μM Mito-CP or Mito-CP-Ac. (*bottom*) Densitometric analysis of replicate immunoblots obtained after stimulation for 5

min with either Mito-CP or Mito-CP-Ac. *- $p < 0.05$ vs. unstimulated controls (Un). Cells stimulated with oligomycin served as a positive control (+). Data shown are the mean ± SD, n = 3.

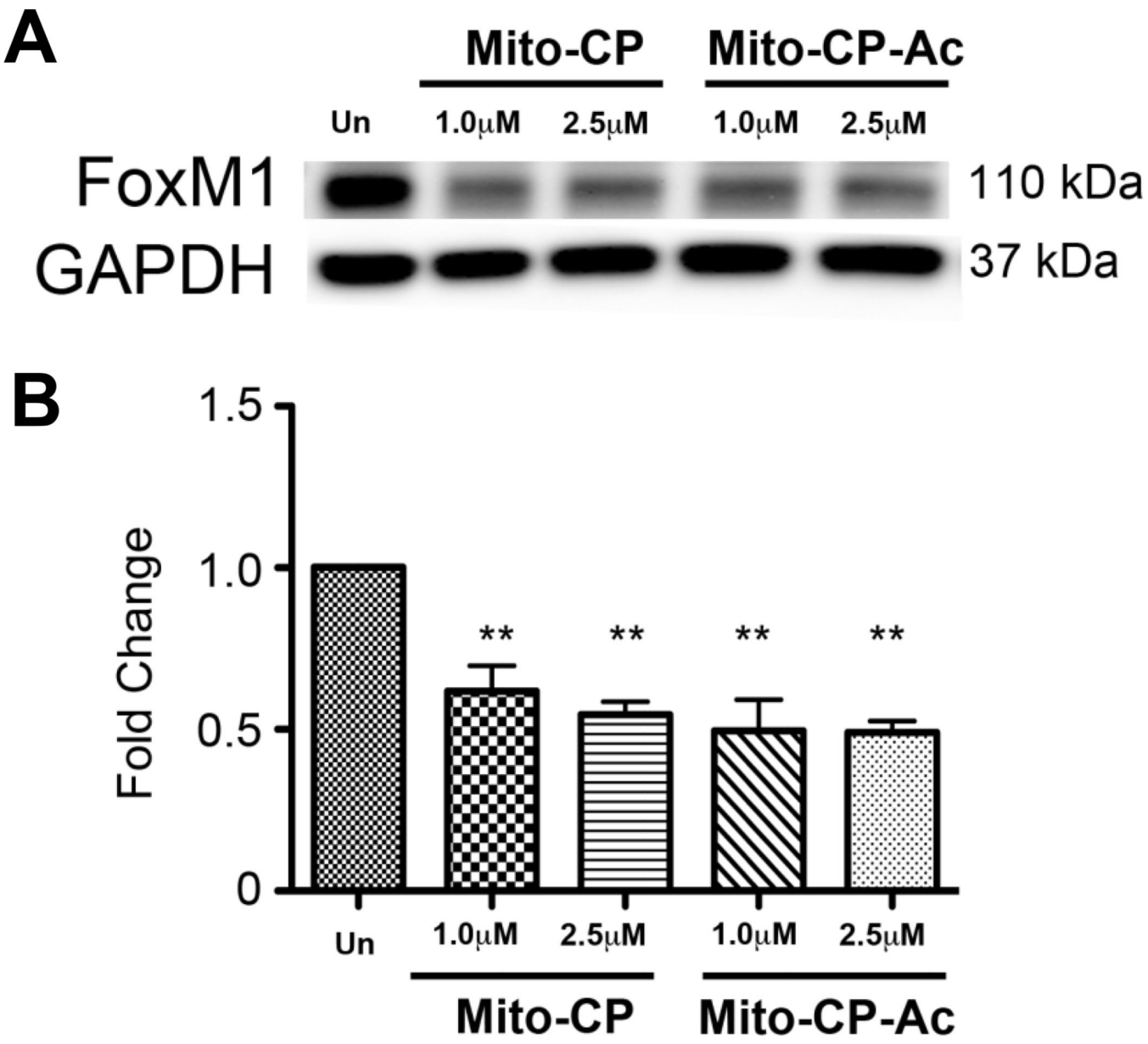

Fig. 7. Effect of Mito-CP and Mito-CP-Ac on activation of FOXM1 in MiaPaCa-2 cells

(A) The representative blot of three independent biological replicates of lysates obtained from MiaPaCa-2 cells stimulated for 12 h with indicated doses of Mito-CP or Mito-CP-Ac. (B) Densitometric analysis of replicate immunoblots obtained with either Mito-CP or Mito-CP-Ac. **- $p < 0.01$ vs. unstimulated controls (Un). Data shown are the mean ± SD, n = 3.